ACTA ASTRONOMICA
Vol. **33** (1983) No 3-4

A Working Model of Sunspot Structure in Photosphere, Chromosphere and Corona, Derived from X-Ray, EUV, Optical and Radio Observations

by

J. Staude[a], F. Fürstenberg[b], J. Hildebrandt[a], A. Krüger[b]

Central Institute for Solar-terrestrial Physics (Heinrich Hertz Institute), Academy of Sciences of the G.D.R.
[a]Solar Observatory Einsteinturm, Potsdam, [b]Berlin-Adlershof

J. Jakimiec

Astronomical Institute of the Wrocław University, Wrocław

V. N. Obridko

Institute of Terrestrial Magnetism, Ionosphere and Radio Wave Propagation, Academy of Sciences of the USSR, Moscow

M. Siarkowski, B. Sylwester and J. Sylwester

Space Research Centre of the Polish Academy of Sciences, Wrocław

Received November 16, 1982; final version received in May 1983

ABSTRACT

Recent high-resolution observations in different spectral ranges, particularly those made for regions inside and above large sunspot umbrae, have been used to study possible interpretations of the observed emissions. The lower umbral chromosphere was found to be best represented by a model similar to that of Teplitskaya *et al.* (1978). The model has been extended to higher levels by a steep gradient of the temperature T, reaching values of $T \approx 40000$ K and electron density $n_e \approx 4 \times 10^{10}$ cm^{-3} at a height of $z \approx 2000$ km above the umbral photosphere; these values are mainly suggested by EUV data from HRTS. At higher levels at least two components must be assumed: The hot component occupying a fraction of $a \approx 0.8$ to 0.9 of the involved volume has a shallow transition layer and coronal values of $T \approx 1.8 \times 10^6$ K and $n_e \approx 10^9$cm^{-3} already at $z \approx 3000$ km to 5000 km. These values are consistent with both the missing X-ray flux above large umbrae and the high brightness temperature of $T_b \approx 1.8 \times 10^6$ K emitted at cm wavelengths from the same place. This hot coronal matter encloses the feet of cold loops which start in a bundle from the

umbra and emit the observed EUV lines at $10^4 \leqslant T \leqslant 10^6$ K. In the corona the z-dependence of all physical quantities including α must be considered as being small over distances of several 10^3 km. Along the loop axis T slowly increases, the loops become more horizontal and appear as hot X-ray loops at distances and heights of several 10^4 km above the plage region.

The model assumptions have been tested and corroborated by recently published observations with high spatial resolution obtained in the X-ray and EUV spectral range from Skylab, HRTS, and SMM, at centimeter wavelengths from RATAN, VLA, and WSRT, and by ground-based magnetograms.

1. Introduction

The present paper summarizes the outcome of a workshop on solar active regions held at the Astronomical Institute of the University of Wrocław, Poland, from 28 November to 6 December, 1979, where a small group of solar physicists from several observatories met to study possible interpretations of the observed emission from inside and above sunspot umbrae at different wavelengths. Preliminary results were presented at two meetings (Bromboszcz *et al.* 1981a, b). The work was continued during a working session held at the Astronomical Observatory Ondrejov from 28 September to 3 October, 1981. Some main conclusions from these meetings and intermediate work are summarized here, while further detailed results are planned to be published in separate papers (cf. also Bromboszcz *et al.* 1982).

More than a decade ago Livshits *at al.* (1966) proposed a model of the atmospheric layers above sunspots. It assumes a transition layer starting in the umbral chromosphere at a height z of about 2000 km above the photosphere and approaching coronal values of the electron temperature $T > 10^6$ K well below 10^4 km. This model could explain the observed microwave spectrum of the S-component from sunspots due to gyromagnetic emission as main contribution to the emission of the S-component in strong magnetic fields. Later on new observations became available including data with high spatial resolution in X-and EUV-lines obtained from Skylab (Foukal *et al.* 1974, Foukal 1975, 1976, 1978, Levine and Withbroe 1977, Cheng and Moe 1977) and HRTS (Brueckner *et al.* 1977, Nicolas *et al.* 1979, Basri *et al.* 1979), but also at centimetric radio wavelengths from solar eclipse observations (Gelfreikh and Kerzhavin 1975). Soon it became clear that these data cannot be explained simultaneously in the frame of a homogeneous model with plane-parallel stratification of the atmosphere above the sunspot umbra. Therefore, Obridko (1979) proposed a new two-component model consisting of cold and hot elements (loops), the fraction of cold elements decreasing with height. This model seemed capable to solve most of the difficulties which arise from attempts to interprete observations at different wavelengths by means of a homo-

geneous model. But objections even to this model were raised from the knowledge of afterwards published observations of large sunspots at X- and centimeter wavelengths (Pallavicini *et al.* 1979) which stimulated our discussion very much. Recently new observations with high spatial resolution at X-ray and EUV wavelengths (see *e.g.* the Proceedings of the Sunspot Workshop: Cram and Thomas 1981) and in the microwave range became available which render new possibilities to check the correctness of our model assumptions.

In the following sections we shall summarize the constraints to the wanted model given by the observations and shall outline the proposed conception. The model will be supported by first detailed calculations concerning the emission at different wavelength regions. Finally, proposals for further investigations will be given which could help to improve and extend that working model in the future.

2. Proposed umbral model at photospheric and chromospheric levels

Empiric models of the umbral atmosphere seem to be well established at the photospheric level owing to observations in the infrared and visible spectral regions. However, uncertainties increase at larger heigths starting from the temperature minimum. In the following we take as much as possible only observed data from the quoted papers, while model-dependent calculations are carried out by means of own procedures concerning *e.g.* the conversion of different height scales (geometrical height z, optical depths in the continuum at $\lambda_0 = 5000$ Å, τ_0, and at other wavelengths λ, τ_λ, mass scale m, etc.). This treatment enables us to obtain a rather self-consistent model with identical assumptions concerning chemical composition and the methods to solve the equations of state, of hydrostatic equilibrium in the atmospheric layers, deviations from LTE, absorption coefficients, etc., but, of course, small differences relative to originally published partial models may also follow. The temperature T (τ_0) and the electron pressure P_e (τ_0) in the photospheric layers were taken from the sunspot model by Stellmacher and Wiehr (1975). For the low chromosphere different sunspot models have been derived from observations of medium-strong lines, of H_α, and especially from the CaII H and K lines by Baranovsky (1974a, b), Teplitskaya *et al.* (1977, 1978), and Kneer and Mattig (1978). Recently EUV observations with high spatial resolution of $\lesssim 1''$ became available concerning chromospheric lines of CO (Bartoe *et al.* 1978, Jordan *et al.* 1979), H_2 (Jordan *et al.* 1978, Bartoe *et al.* 1979), Ly_α (Basri *et al.* 1979, Kneer *et al.* 1981), and SiIII (Nicolas *et al.* 1979). These data were used to test and extend the existing chromospheric models in order to obtain a working model of the umbra

up to $T \lesssim 40000$ K: The run of $T(z) \leqslant 11000$ K in the model of Teplitskaya *et al.* (1977, 1978) was found to agree best with the new data, while our assumend values of P_e are somewhat larger. (We assumed hydrostatic equilibrium taking into account a turbulent pressure $P_{tu} = \varrho v^2/2$ where ϱ is the mass density and v — the turbulent velocity; Teplitskaya *et al.* tried to determine the electron density $n_e = P_e/(kT)$ from observations without assuming hydrostatic equilibrium; k is the Boltzmann constant.)

Our extension towards larger z and T results in a steep gradient of $T(z)$ which is at least twice the size of that in facular points and much larger than in the undisturbed Sun; values of n_e at equal T have been found between those of facular points and bright network points of the quiet chromosphere. A list of the model is given in Table 1.

Table 1

Umbral Model — photosphere and chromosphere

z/km	T/K	n_e/cm^{-3}	$\varrho/(g \cdot cm^{-3})$
1902.0	4.2 E+4	3.800 E+10	8.425 E-14
1901.6	3.8	4.145	9.507
1901.0	3.2	4.591	1.174 E-13
1900.4	2.6	4.416	1.602
1900.0	2.2	3.474	2.119
1870	2.1 E+4	4.946 E+10	2.139 E-13
1860	2.0	4.862	2.318
1840	1.8	5.605	2.586
1810	1.6	6.970	2.923
1775	1.4	9.121	4.722
1745	1.2 E+4	6.594 E+10	6.931 E-13
1720	1.0	3.829	9.970
1695	9.0 E+3	4.824	1.209 E-12
1640	8.0	6.228	1.712
1515	7.0	7.643	3.661
1480	6700	5.209 E+10	4.641 E-12
1400	6250	4.121	7.620
1290	5700	3.537	1.558 E-11
1200	5000	7.740 E+9	2.947
1130	4500	2.661	3.846
1050	4000	2.388 E+9	5.570 E-11
900	3500	3.464	1.331 E-10
800	3250	2.898	2.403
650	3100	3.311	6.508
500	3000	6.266	2.563 E-9
298.0	3091	4.591 E+10	2.738 E-8
231.3	3193	1.083 E+11	6.462
167.6	3341	3.224	1.877 E-7
103.2	3523	8.605	4.410
35.8	3769	2.489 E+12	9.829
0.0	3964	4.775 E+12	1.410 E-6
-37.5	4350	1.260 E+13	1.847
-77.2	5400	5.833	2.041
-115.4	6810	3.688 E+14	2.106
-132.9	8520	3.693 E+15	1.850

The reference model of the mean undisturbed photosphere and chromosphere was calculated using the same procedures as those for the sunspot model but adopting T (m) from papers by Ayres and Linsky (1976) and Basri *et al.* (1979), while the extension to the subphotospheric layers in both models was already obtained by earlier model calculations for

the convective zone (Staude 1976, 1978). The resulting models representing the lower boundary conditions for our further calculations and discussion are given in Fig. 1. Here the zero point of the z-scale was chosen in such

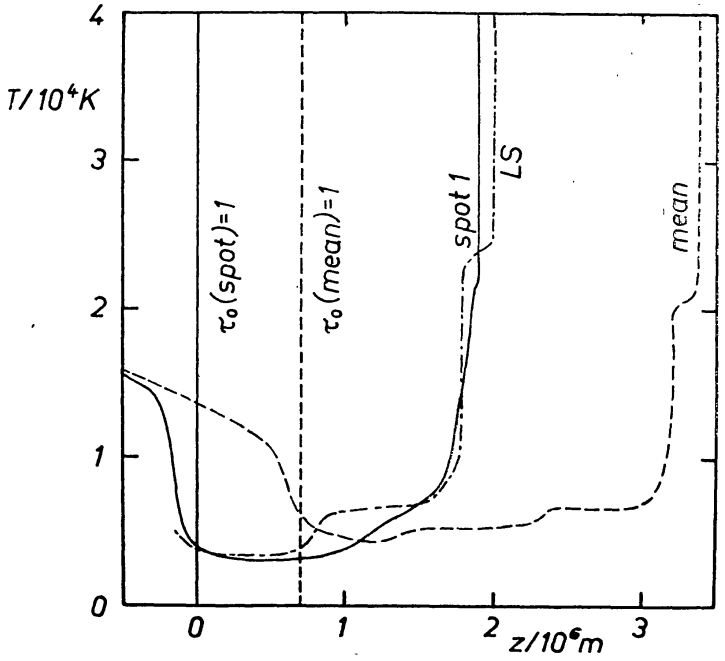

Fig. 1a. Temperature T *vs.* geometrical height z for our sunspot model (full line), the mean undisturbed Sun (dashed line), and the sunspot model of Lites and Skumanich (LS, dash-dot line) for comparison.

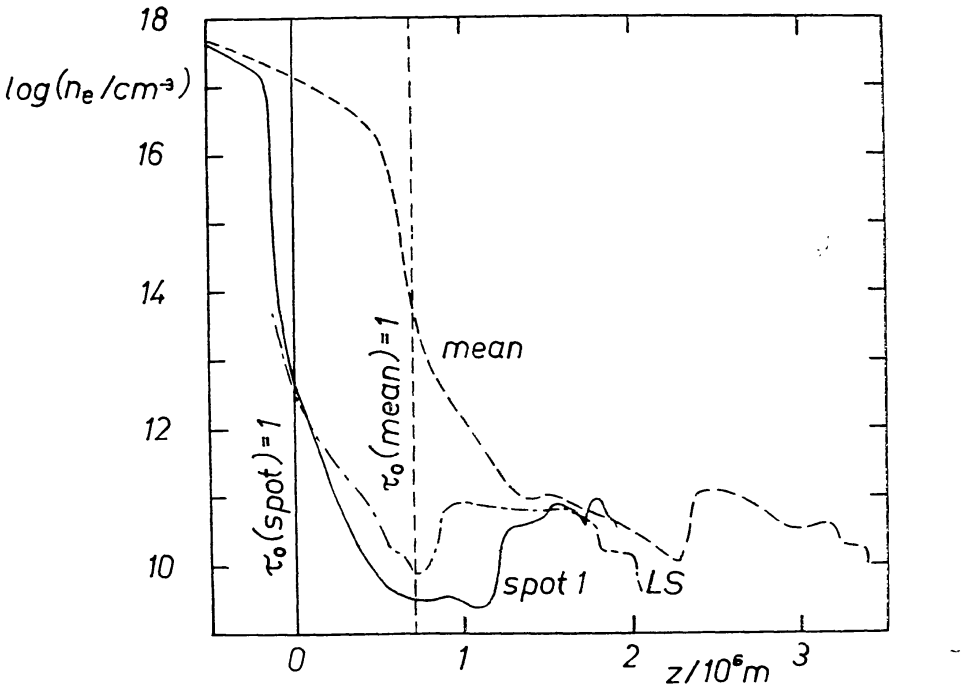

Fig. 1b. Electron density n_e *vs.* geometrical height z. Symbols like in Fig. 1a.

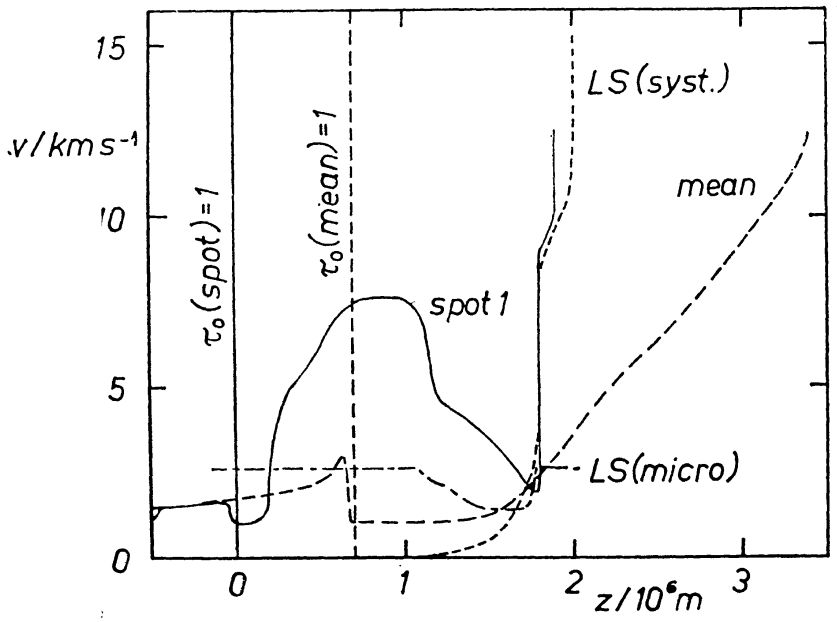

Fig. 1c. Turbulent velocity v *vs.* geometrical height z. Shortly dashed line represents a systematic velocity not taken into account in the turbulent pressure. Other symbols like in Fig. 1a.

a way that a Wilson depression of 700 km is taken into account ($z = 0$ at $\tau_0 = 1$ in the umbra, $z = 700$ km at $\tau_0 = 1$ in the undisturbed photosphere). Then the mass densities ϱ in both models coincide at $z = 0$ as it has been suggested by Maltby (1977). More details on this part of the model calculations and the used procedures and assumptions were published elsewhere (Staude 1981), while a preliminary version of the models has been used already in another paper (Staude 1980). Afterwards analogous model calculations have been carried out also for a plage model and for several variants of umbral models assuming different extents and therefore also different densities n_e and different gradients of T (figures of such models can be found in a paper by Žugžda *et al.* 1983); also various models of $v(z)$ have been tested. Full numerical tables of such models have been published in a recent paper by Staude (1983) where also the used computer programs are described in detail.

Meanwhile a complete chromospheric umbral model has also been derived by Lites and Skumanich (1982), hereafter referred to as LS; the $T(z)$ from this model has been adopted by Avrett (1981) for his reference model atmosphere calculations resulting in the Sunspot sunspot model. Figs. 1 include the LS model for comparison with our model: Fig. 1a shows that $T(z)$ is similar in both models, but some differences are introduced by the assumption of 2 plateaus of T in the LS model resulting in higher values of T in the lower chromosphere but somewhat smaller T in the upper chromosphere; consequently the same is valid

for n_e (Fig. 1b). The assumed run of $v(z)$ is given in Fig. 1c: Only the fraction labelled 'micro' has been taken into account in P_{tu} for the LS model, but the fraction of systematic velocity ('syst.') is close to our assumed $v(z)$ in the upper chromosphere. In another recent model of the lower umbral chromosphere (Yun *et al.* 1981, Beebe *et al.* 1982) the extent of the chromosphere is much smaller, therefore T and n_e are larger than in the models discussed above. Nicolas *et al.* (1982) derived P_e values for the upper umbral chromosphere and transition region; these values are 2 to 3 times larger than those in our original model but about 10 times larger than those in the LS model.

3. Extension of the model towards the transition layer and corona

In a paper by Pallavicini *et al.* (1979) high-resolution X-ray images from Skylab (2″ resolution, 2-60 Å spectral range) are compared with radio data obtained with the Stanford interferometer (spatial resolution 16″ in one direction) at 2.8 cm wavelength. Hence two features are to be noted:

Firstly, as expected, increased microwave emission is observed above plage areas with brightness temperatures of $T_b \approx 2 \times 10^5$ K; on the disk these regions coincide with those of increased X-ray emission. The interpretation of these emissions seems to be quite straightforward as pointed out by the authors: The X-rays are emitted from hot loops above the plage areas ($T \approx 2.5 \times 10^6$ K, $n_e \approx 10^9 \ldots 10^{10}$ cm^{-3}). These regions are optically thin and negligible at microwaves since the magnetic fields are not sufficient to emit thermal gyromagnetic emission. For thermal bremsstrahlung, on the other hand, the main microwave flux originates deeper in the atmosphere where the temperatures are much lower. It should be mentioned, however, that in a recent paper Kundu *et al.* (1980) gave evidence for gyroresonance absorption at the apex of hot loops. This result was obtained from 3.7 and 11 cm radio maps with resolutions of $1''.5 \times 3''.4$ and $4''.6 \times 10''.2$, respectively, EUV spectroheliograms, and X-ray photographs. The observed $T_b \approx (2.4\text{-}3.0) \times 10^6$ K from the maximum radio emission agreed with the T values derived from the X and EUV data. The derived field strengths of $B \approx 300$ G at heigths of some 10^4 km are compatible with our earlier force-free magnetic field extrapolations from active regions with large sunspots (Seehafer and Staude 1979, 1980). There is no agreement, however, concerning the extent of such an interpretation: Felli *et al.* (1981) used VLA observations of plages at 6 cm (intensity I and circular polarization V) and derived $T \approx 2.5 \times$ $\times 10^6$ K, $n_e \approx 5 \times 10^9$ cm^{-3}, $B \approx 250$ G assuming thermal bremsstrahlung comprising the vast majority of 6 cm flux from active regions. On the

other hand, according to Schmahl *et al.* (1982) gyroresonance absorption at low harmonics ($B \approx 600$ G for the 3rd harmonic) is the main mechanism for the bulk of the 6 cm emission.

Secondly, the picture is more complicated above or close to the central regions of large sunspots: Here the peaks of radio flux with $T_b \approx 1.8 \times 10^6$ K coincide with holes in the X-ray emission (Pallavicini *et al.* 1979), contrary to the surrounding plage area. A hint for reduced X-ray emission above a large sunspot may be also found in other Skylab data (Pye *et al.* 1978). Calculations for the X-ray emission in the considered spectral range carried out by the Wrocław group result in an upper limit of $T \leqslant \leqslant 2 \times 10^6$ K above sunspots, otherweise X-ray emission should be observed. Model calculations by Gelfreikh and Lubyshev (1979) show that such values could also be compatible with the high-resolution microwave observations: They assumed a simple model of the sunspot corona with $T = 1.8 \times 10^6$ K and $n_e = 2 \times 10^9$ cm^{-3} at $z = z_t = 2000$ km, where z_t is the height of the transition layer between chromosphere and corona above $\tau_0 = 1$. Emission from the transition layer (assumed to be infinitely small) and chromosphere ($T = 0$) were neglected, the magnetic structure of the sunspot was represented by a dipole, and expressions for the optical depths of the gyroresonance levels were taken from Zlotnik (1968), assuming gyroresonance absorption to be the main process responsible for the observed microwave emission in the strong umbral magnetic field. The calculated spectra and spatial distributions of T_b from this model are for the most part compatible with existing observations. Pallavicini *et al.* (1979) sometimes reported values of T_b well above the average value of $T_b = 1.8 \times 10^6$ K, single values ranging from 4×10^5 K up to 4.7×10^6 K. These larger values would be incompatible with the model explaining the missing X-ray emission as well, but the large range of the T_b values is, at least partly, due to uncertainties in the determination of the source size (strong short-term fluctuations of T_b observed from single sunspots support this suspicion), moreover, some of the listed high T_b values are either connected with a non-vanishing X-ray emission or X-ray data have not been published. In recent high-resolution radio observations at 6 cm (Alissandrakis and Kundu 1982, Lang and Willson 1982) rings and horseshoe-like structures have been detected in the maps of the intensity I and circular polarization V which agree with the predictions of the model by Gelfreikh and Lubyshev (1979), however, they are no proof for a strong depression of T or n_e above the umbral centre as it has been sometimes erroneously assumed.

The hitherto outlined model designed for explaining both X-ray and microwave emission is further complicated by the high-resolution EUV observations quoted in Section 1 and showing strongly enhanced line emission directly above umbrae, by contrast to the surrounding plage,

at temperatures of some $10^4 \leqslant T \leqslant 10^6$ K. This means that cool plasma in loops at transition layer temperatures coexists with the hot corona above the umbra, and our model must then be extended to include such inhomogeneous structures. Concerning the different emissions our estimates are supporting the following conception: Starting from values of the mean chromosphere of $n_e \approx 4 \times 10^{10}$ cm^{-3} and $T \approx 40000$ K at $z \approx 2000$ km we have a hot component with a steep transition layer and coronal values of $T \approx 1.8 \times 10^6$ K and $n_e \approx 10^9$ cm^{-3} already at $z \approx 3000$ to 5000 km, occupying a fraction of $a \approx 0.8$ to 0.9 of the volume and enclosing the feet of cold loops which start in a bundle from the umbra. The residual 10 to 20 per cent of cold loop matter renders possible

(*A*) to explain the observed EUV emission measures within the limits of observational errors and

(*B*) to consider the effect of the cold fraction $\beta = (1-a)$ of the volume on the resulting radio flux in a first approximation only as a dilution factor.

In the corona the z-dependence of all physical quantities including a may be considered as being small over distances of several 10^3 km, while strong gradients of T and P_e do exist in horizontal direction, *i.e.* perpendicularly to the magnetic field lines all transport mechanisms are strongly reduced. Along the direction of loops T slowly increases. Those loops reaching greater distances tend to become hotter corresponding to the occurrence of hot loops at distances and heights of several 10^4 km above the plage region. Models of such loops have been discussed *e.g.* by Rosner *et al.* (1979) and by Vesecky *et al.* (1979). The cold H_a loops with inverse Evershed effect representing the superpenumbra (Maltby 1975) are low-lying structures leaving sideward the umbra at low chromospheric levels ($z \approx 2000$ km).

The outlined model is in agreement with latest sunspot investigations: Pallavicini *et al.* (1981) derived a lower limit of $a \gtrsim 0.7$ for most umbrae. The cool loops obviously consist of unresolved filamentary structures; hot loops do not appear to be wrapped around the cooler loops but both are separate structures (Dere 1982, Dere *et al.* 1982, Nicolas *et al.* 1982). Especially the observations during the SMY period are able to corroborate our assumed model parameters: Kingston *et al.* (1982) found values of log ($n_e\, T/K$ cm^{-3}) ≈ 15.0 to 15.3 in the umbral transition region and lower corona. The unexpected high values of $B \approx 1.0$ to 1.4 kG at 10^5 K (Henze *et al.* 1982) indicate a deep-set transition layer at a height of a few 10^3 km. A height of the 6 cm emission of $z = 3.5 \times 10^4$ km above the spot has been derived by Lang *et al.* (1983) from projection effects which would contradict our assumption of a deep-set and thin transition layer, but values of $B \approx 600$ G (900 G) are required to explain the observed I and V data by gyroresonant emission at the 3rd (2nd) harmonic; such an extre-

mely small gradient of B contradicts all existing magnetic field extrapolations (*cf.* Seehafer 1982). At the Crimean SMY Workshop, March 1981, F. Chiuderi-Drago presented a compilation of observation of AR 2490 from June 10, 1980, including high-resolution radio maps at 2 cm (I from VLA) and 6 cm (I and V from WSRT), and spectroheliograms in C IV and X-ray lines from the UVSP and XRP instruments onboard SMM, respectively (Chiuderi-Drago *et al.* 1982). The strong and polarized 6 cm radiation but missing or only weak emission at the other wavelengths near a sunspot group, contrary to the plage region, support the proposed model with a shallow transition layer and the absence of plasma with $T > 2 \times 10^6$ K above sunspots.

A well defined quantitative model with $T(z)$ and $n_e(z)$ extended above the upper boundary of our original mode ($T = 40000$ K, see Section 2) may be obtained by assuming:

(A) hydrostatic equilibrium and

(B) a constant conductive heat flux F_c in the transition region (*cf.* Alissandrakis *et al.* 1980), or $P_e = \text{const.}$ instead of $F_c = \text{const.}$ Values of P_e and $\mathrm{d}T/\mathrm{d}z$ for different values of T have been derived by Nicolas *et al.* (1982) assuming a filling factor of $\beta = 1.0$ for the EUV emission. If we assume a smaller value, say $\beta = 0.1$, the value of P_e would hardly

Table 2

Hot component ($\alpha = 0.9$), $F_c = 10^7$ erg cm^{-2} s^{-1}

z/km	T/K	n_e/cm^{-3}
1903.00	5.000 E+4	3.170 E+10
1903.05	8.607	1.841
1903.10	1.026 E+5	1.544
1903.25	1.314	1.206
1903.50	1.594	9.939 E+9
1903.75	1.787 E+5	8.866 E+9
1904.0	1.939	8.173
1904.5	2.175	7.285
1905.0	2.361	6.712
1906.0	2.649	5.980
1908	3.065 E+5	5.169 E+9
1910	3.374	4.695
1915	3.935	4.025
1920	4.346	3.643
1930	4.960	3.190
1950	5.811 E+5	2.721 E+9
1970	6.430	2.457
2000	7.147	2.209
2100	8.751	1.800
2200	9.840	1.597
2300	1.069 E+6	1.467 E+9
2500	1.201	1.301
2750	1.327	1.173
3000	1.429	1.085
3250	1.516	1.020
3500	1.591 E+6	9.628 E+8
3750	1.659	9.259
4000	1.720	8.902
4362	1.800	8.471
4500	1.828	8.327

Table 3

Cold component ($\beta = 0.1$), $F_c = 10^4$ erg cm^{-2} s^{-1}

z/km	T/K	n_e/cm^{-3}
1903	5.000 E+4	3.170 E+10
1910	5.911	2.674
1920	6.801	2.317
1930	7.469	2.104
1950	8.479	1.844
1970	9.255 E+4	1.682 E+10
2000	1.018 E+5	1.519
2050	1.137	1.348
2100	1.231	1.234
2200	1.379	1.085
2300	1.495 E+5	9.868 E+9
2500	1.676	8.579
2750	1.850	7.553
3000	1.990	6.837
3500	2.214	5.858
4000	2.393 E+5	5.188 E+9
5000	2.674	4.287
7000	3.082	3.233
1.0 E+4	3.517	2.358
1.5 E+4	4.034	1.574
2.0 E+4	4.424 E+5	1.130 E+9
3.0	5.017	6.497 E+8
5.0	5.849	2.652
7.0	6.460	1.246
1.0 E+5	7.170	4.612 E+7

be influenced (it has been determined from intensity ratios of lines which are formed at nearly equal values of T) but dT/dz and hence F_c would be reduced by one order of magnitude in the cold elements which emit the bulk of EUV lines and appear as cool "plumes" above the umbra. For the remaining fraction $\alpha = 1-\beta$ of the atmosphere, however, the assumption of large values of dT/dz and F_c, that is a thin and deep transition region as it has been outlined above, seems to be justified and compatible with all available observations. Such models of the hot and cold components are listed in Tables 2 and 3.

4. Model of X-ray emission

High-resolution X-ray pictures, made from Skylab, showed that steady-state loops connecting main sunspots of an active region are the dominant features of the coronal active regions in that spectral region. An example of such loops was comprehensively investigated by Pye *et al.* (1978) (*cf.* loops Nos. 2-5 in their Figure 9).

The Skylab pictures are known to be not very suitable for investigation of the temperature structure of the emitting feature (*cf.* the discussion on pages 126 and 132 in the paper by Pye *et al.*). Nevertheless, their ana-

lysis of the Skylab photographs in terms of temperature distribution suggests that:

(*A*) the material of the loops seen in the Skylab pictures obtained with filter No. 1, is at temperatures of $T = 2.5 \times 10^6$ K (*cf.* Fig. 6 in that paper);

(*B*) there is some gradual decrease of the temperature towards the footpoints of the loops.

The temperature structure of the active region loops is investigated more adequately from more narrow band observations. Parkinson (1973) used OSO-5 soft X-ray observations of limb transits of coronal active regions as well as rocket spectral observations to investigate the height structure of the regions. He derived the well-known picture of the loop--like structure connecting the main sunspots. An individual loop of this structure is hottest at the top (*i.e.* between the sunspots) and the temperature gradually decreases in the lower part of the loops (legs) (*cf.* Fig. 4 in Parkinson's paper).

Jakimiec *et al.* (1978) investigated a large, hot postflare loop observed on 10 February 1972 by GSFC spectrometer onboard OSO-7. The observations allowed to construct a map of the temperature distribution, and gradual decrease of the temperature along the legs of the loop is seen from the map. In the present paper we investigated the temperature distribution along the active region X-ray loops using the unique data presented in the paper by Pye *et al.* (1978). It is important that in that paper not only the Skylab X-ray photographs, but also X-ray spectra simultaneously obtained with a rocket-borne spectrometer, are given. The geometry of the active region X-ray loops can be specified from the high-resolution Skylab photographs and the temperature structure of the loops can be determined using the X-ray spectra.

As it is shown in that paper by Pye *et al.* (1978), four X-ray loops, connecting the main spots of the active region (loops Nos. 2-5 in their Figure 9a) give dominant contribution to the recorded X-ray spectra. These four loops are very similar in dimensions and X-ray brightness, therefore we have investigated a "mean" loop, defined as an average of the four loops. The measured distance between the footpoints of the loop is 1.12×10^5 km, an estimated height of the loop is 3×10^4 km, and we assume that the loop emits 1/4 of the flux recorded in each of the six investigated X-ray lines (Table I in the paper by Pye *et al.* 1978).

From these line intensities we have calculated the differential emission measure (DEM) distribution, $\varphi(T)$, for the mean loop. The calculations were carried out using the modified Withbroe iterative procedure (Sylwester *et al.* 1980). The resulting DEM distribution is shown in Fig. 2.

Next we have assumed, following Withbroe (1978), that the temperature changes are significant only along the loop, *i.e.* that we can consider the

temperature as a function of s only where s is a coordinate along the loop axis. The definition of the DEM can be written as follows:

$$\varphi(T)\mathrm{d}T = n_e^2 \mathrm{d}V,$$

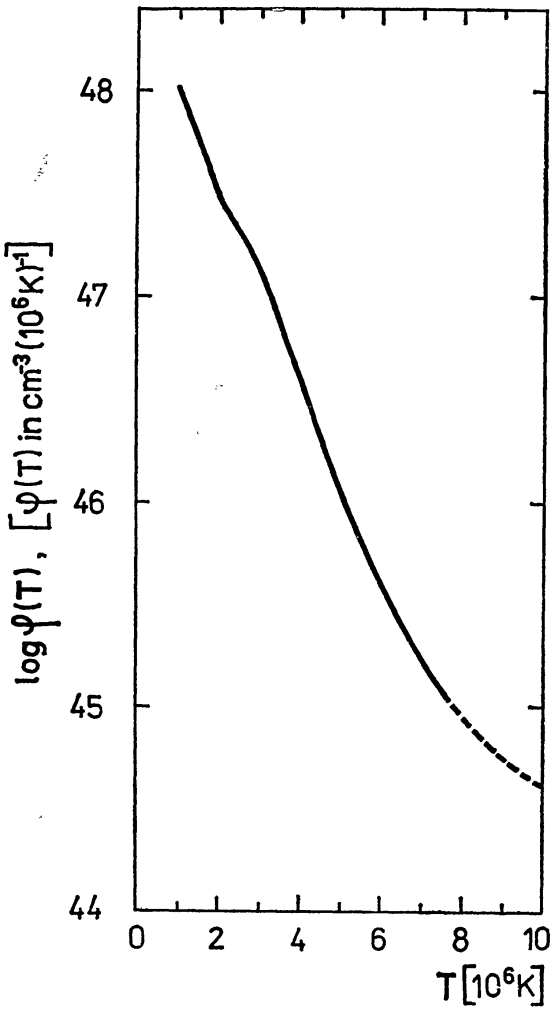

Fig. 2. The differential emission measure distribution in a typical active region X-ray loop as observed by Pye *et al.* (1978).

where n_e is the number electron density and $\mathrm{d}V$ is the volume of plasma being at a temperature between T und $T+\mathrm{d}T$.

Introducing the gas pressure:

$$p = 2n_e kT$$

and writing

$$\mathrm{d}V = A(s)\mathrm{d}s,$$

where $A(s)$ is the cross-section of the investigated tube, we obtain the following equation:

$$\frac{dT}{ds} = \left(\frac{p}{2kT}\right)^2 A(s) \frac{1}{\varphi(T)}.$$

Integrating this equation under simplifying assumptions: p = const., A = const., we have obtained the temperature distribution function $T(s)$ as shown in Fig. 3 (solid line). For comparison we show in Fig. 3

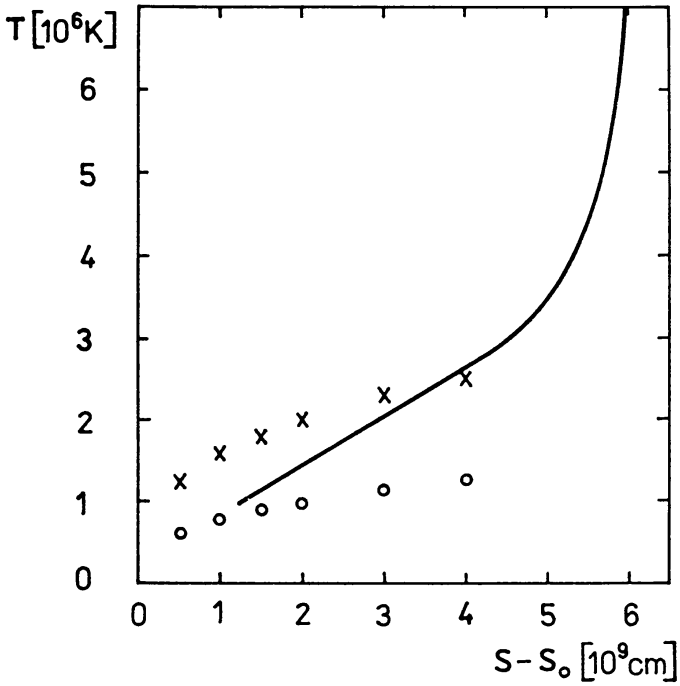

Fig. 3. Distribution of the temperature along the active region X-ray loop. s is the coordinate along the loop, s_0 is located at the footpoint of the loop. Solid line shows the empirical model of the typical loop as observed by Pye *et al.* (1978) Points indicate theoretical models of active region loops (Rosner et al. 1978). Models for the following values of the gas pressure are shown: × — for $p = 10^{-5}$ Ncm^{-2}, ○ — for $p = 10^{-6}$ Ncm^{-2}.

also the temperature distribution along the theoretical models of steady-state, p = const., flux tubes taken from the paper by Rosner *et al.* (1978).

It is seen from Fig. 3 that the temperature gradients should be low, indeed, in the legs of the loops, so that in the lower parts of the loop, up to the height of a few tens of thousands of kilometers, the temperature may easily be not higher than 2×10^6 K as proposed in our model.

5. Modelling of the S-component of radio emission

The microwave emission from active regions (S-component) can be regarded as an independent opportunity of checking the present model assumptions at different height levels. For this reason an emission model of the S-component has been developed which is described in more detail elsewhere (Krüger *et al.* 1983). Earlier models were described by several authors (*e.g.* Lantos 1968, Zlotnik 1968).

The present model permits the calculation of brightness distribution across local sources of the S-component at any given fixed frequency. The calculations are performed for both magnetoionic wave modes by solving the equation of radiative transfer along straight ray trajectories thus yielding information about total flux and polarization characteristics. Thermal bremsstrahlung and gyromagnetic radiation were taken as the relevant emission processes.

Input quantities for the numerical computations are threedimensional fields of temperature, electron density, and the magnetic vector. As a first

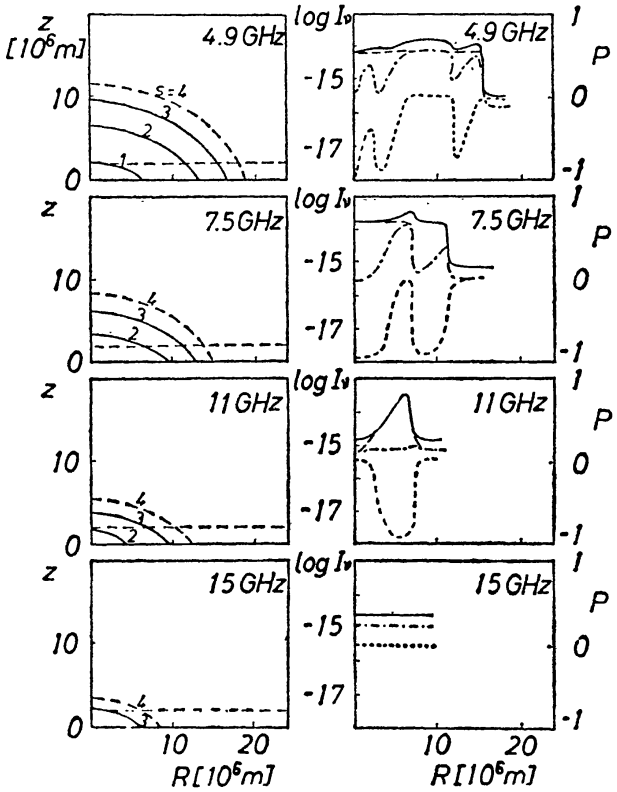

Fig. 4. Intensity distribution (right) of a cylindric source model of the S-component (magnetic dipole 1.5×10^7 m below the photosphere reaching $B_{max} = 2500$ G at the photosphere, n_e and T distributions according to the model of Fig. 1 for different microwave frequencies) in comparison with the position of gyroresonance layers (left) in the corona. Full line — total intensity, dash-dot line — ordinary wave, dotted line — degree of polarization, dashed line — extraordinary wave.

step a cylindric-symmetric structure of these three basic quantities was presumed whereas temperature and density were adopted from the model shown in Fig. 1 and extrapolated towards larger heights by assumption of hydrostatic equilibrium and a constant conductive flux F_c. Here only F_c or the thickness of the transition layer remains as a free parameter (*cf.* Alissandrakis *et al.* 1980, and Section 3 above). We assumed $F_c = 10^7$ erg·cm^{-2} s^{-1} for the present sample calculation.

As an example in Fig. 4 the computed cross-sections of brightness and the degree of polarization over the core region of a sunspot were obtained for various frequencies (which are in our case operating frequencies of the radio telescopes RATAN and VLA). The magnetic field model used here was one pole of a magnetic dipole. The field depends essentially on two parameters, the maximum field B_{max} at the centre of the bottom of the considered source volume ($R = 0$) and the height scale of field decrease. Since the resulting radiation strongly depends on the actual magnetic field distribution, a number of test calculations was carried out with different magnetic field parameters simulating solar activity at different stages of its development. Fig. 5 shows resulting spectra of flux density, effective source radii, and the degree of polarization for different values of B_{max} and two characteristic height scales, providing a sensitive tool for the diagnostics of regular spotgroups.

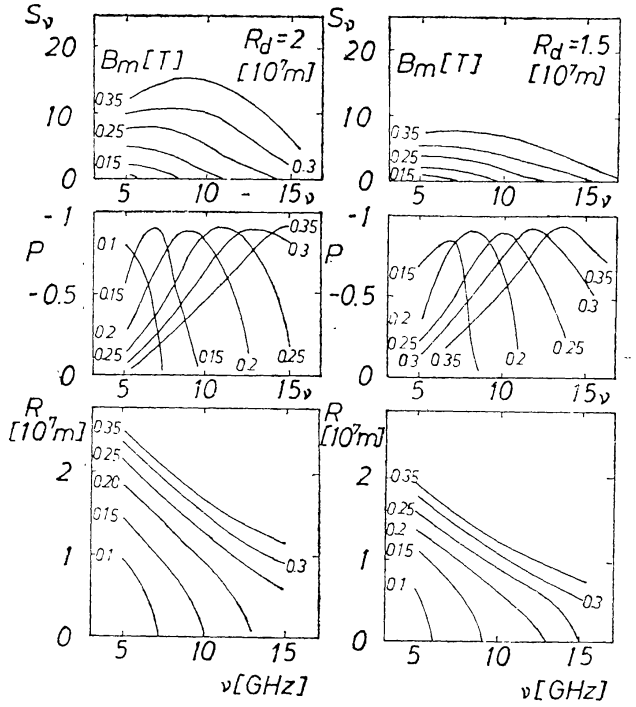

Fig. 5. Calculated spectra of flux density (top), degree of polarization (middle), and effective source radii for different assumed values of B_{max} and depths R_d of the magnetic dipole below the photosphere (other conditions the same as for Fig. 4).

Though detailed comparisons with observational results are yet up to a future work, the general tendency coming out from the calculations is promising. In particular, a lower boundary of the corona at heights of the order of 2000 km above the photosphere may well explain a number of observational features discussed above. The content of cool matter indicated by EUV and H_a fine structures may not exceed 10 per cent in the considered frequency range and was therefore not taken into account by the orientating calculations of the radio model.

First applications of the microwave emission model were made with respect to RATAN 600 observations and measurements in the mm-range (Akhmedov *et al.* 1982, Urpo *et al.* 1983). Hence preliminary results refer to the derivation of the height scale of the magnetic field above sunspot umbrae and the degree of inhomogeneity of plage structure seen at mm-waves. As a next step the incorporation of force-free extrapolated magnetic fields from real magnetograms into the S-component emission model is under way.

6. Conclusions

The presented sunspot model consists of several parts which have been consistently put together:

— the umbral model describing the spatial distribution of thermodynamic quantities up to the transition region as derived from EUV and optical observations,
— the magnetic field model,
— the model of X-ray emission, and
— the S-component emission model.

Our preliminary estimates of the emission at different wavelength regions have shown that the discussed sunspot model is able to interprete the basic features of presently available observations. Of course, this conclusion must be further corroborated by more exact model calculations, to begin with computations for the radiation at EUV and X-ray as well as at radio frequencies. Moreover, the magnetic field model should be improved by applying real magnetic field distributions obtained by force-free field extrapolations from photospheric magnetograms. Finally, the analysis should be extended to greater parts of an active region including the plage region and active region coronal loops. Several of those proposed steps are being prepared.

Semi-empirical working models such as the present one are required in order to study other physical processes in sunspots, *e.g.* the propagation and dissipation of hydromagnetic waves and oscillations. Such work has been done in a recent paper by Žugžda *et al.* (1983) using the present sunspot model.

In order to test and improve our sunspot working model it would be highly desirable to have better observed data from active regions including large sunspots. Such measurements should be obtained with high spatial resolution and simultaneously (to eliminate errors due to differences between individual sunspots) at many different wavelengths from radio waves down to X-rays. Coordinated simultaneous observations, including microwave data from large radio telescopes such as RATAN, VLA, and WSRI, EUV and X-ray data as well as groundbased magnetic field measurements, that is an integrated campaign similar to that during the SMY, would be of high value.

Acknowledgments. V. N. Obridko, A. Krüger, and J. Staude wish to thank the University of Wrocław for the invitation and to thank the Wrocław colleagues, especially Maria and Jerzy Jakimiec, for their hospitality during the workshop in 1979 which initiated the present work. F. Chiuderi-Drago kindly sent us copies of the data which she compiled from AR 2490 for June 10, 1980. In carrying out this work, the authors have benefited considerably from their participation in the SMY Workshop held at the Crimean Astrophysical Observatory, USSR, in March 1981. This Workshop was supported by SCOSTEP and the USSR Academy of Sciences.

The participants of the working session in 1981 would like to express their thanks to the colleagues of the Ondrejov Observatory, particularly Prof. V. Bumba, Prof. M. Kopecký, and Dr. P. Ambroz for hospitality.

REFERENCES

Akhmedov, S. B., Gelfreikh, G. B., Krüger, A., Fürstenberg, F., and Hildebrandt, J., 1982, *Soln. dannye*, **10**, 72.

Alissandrakis, C. E., Kundu, M. R., and Lantos, P., 1980, *Astron. Astrophys.*, **82**, 30.

Alissandrakis, C. E., and Kundu, M. R., 1982, *Astrophys. J.*, **253**, L 49.

Avrett, E. H., 1981, in: L. E. Cram and J. H. Thomas (eds.), *The Physics of Sunspots*, p. 235.

Ayres, T. R., and Linsky, J. L., 1976, *Astrophys. J.*, **205**, 874.

Baranovsky, E. A., 1974a, *Izv. KrAO*, **49**, 25.

— 1974b, ibid., **51**, 56.

Bartoe, J.-D. F., Brueckner, G. E., Nicolas, K. R., Sandlin, G. D., Van Hoosier, M. E., and Jordan, C., 1979, *Monthly Notices Roy. Astron. Soc.*, **187**, 463.

Bartoe, J.-D. F., Brueckner, G. E., Sandlin, G. D., and Van Hoosier, M. E., 1978, *Astrophys. J.*, **223**, L 51.

Basri, G. S., Linsky, J. L., Bartoe, J.-D. F., Brueckner, G. E., and Van Hoosier, M. E., 1979, *Astrophys. J.*, **230**, 924.

Beebe, H. A., Baggett, W. E., and Yun, H. S., 1982, *Solar Phys.*, **79**, 31.

Bromboszcz, G., Jakimiec, J., Siarkowski, M., Sylwester, B., Sylwester, J., Obridko, V. N., Fürstenberg, F., Hildebrandt, J., Krüger, A., and Staude,

J., 1981a, *Proc. X Consultation on Solar Physics at Potsdam, 1980, Physica Solariterr.*, **16**, 155;
— 1981b, *Proc. SMY Workshop, Crimea, March 1981*, Vol. 1, p. 224;
— 1982, IZMIRAN (Moscow) Preprint No. 11a.
Brueckner, C. E., Bartoe, J.-D. F., and Van Hoosier, G. E., 1977, *Proc. of the November, 1977 OSO-8 Workshop, Boulder, Colorado*, p. 380.
Cheng, C.-C., and Kjeldseth-Moe, O., 1977, Solar Phys., **52**, 327.
Chiuderi-Drago, F., Bandiera, R., Falciani, R., Antonucci, E., Lang, K. R., Willson, R. F., Shibasaki, K., and Slottje, C., 1982, *Solar Phys.* **80**, 71.
Cram, L. E., and Thomas, J. H. (eds.)., 1981, *The Physics of Sunspots*, Proc. of the Sunspot sunspot Workshop, Sacramento Peak Observatory Conference, 14-17 July 1981.
Dere, K. P., 1982, *Solar Phys.* **75**, 189.
Dere, K. P., Bartoe, J.-D. F., and Brueckner, G. E., 1982, *Astrophys. J.*, **259**, 366.
Felli, M., Lang, K. R., and Willson, R. F., 1981, *Astrophys. J.*, **247**, 325.
Foukal, P. V., 1975, *Solar Phys.*, **43**, 327.
— 1976, *Astrophys. J.*, **210**, 575.
— 1978, *ibid.*, **223**, 1046.
Foukal, P. V., Huber, M. C. E., Noyes, R. W., Reeves, E. M., Schmahl, E. J., Timothy, J. G., Vernazza, J. E., and Withbroe, G. L., 1974, *Astrophys. J.* **193**, L 143.
Gelfreikh, G. B., Korzhavin, A. N., 1976, in *Fizika solnechnikh pyaten*, Proc. VIII Consultation on Solar Physics at Irkutsk, Nauka, Moskva, p. 94.
Gelfreikh, G. B., Lubyshev, B. I., 1979, *Astron. Zh.*, **56**, 562.
Henze, Jr., W., Tandberg-Hanssen, E., Hagyard, M. J., Woodgate, B. E., Shine, R. A., Beckers, J. M., Bruner, M., Gurman, J. B., Hyder, C. L., and West, E. A., 1982, *Solar Phys.*, **81**, 231.
Jakimiec, J., Neupert, W. M., Sylwester, B., and Sylwester, J., 1978, paper presented at the IX Consultation on Solar Physics, to be submitted to Solar Phys.
Jordan, C., Bartoe, J.-D., F., Brueckner, G. E., Nicolas, K. R., Sandlin, G. D., and Van Hoosier, M. E., 1979, *Monthly Notices Roy. Astron. Soc.*, **187**, 473.
Jordan, C., Brueckner, G. E., Bartoe, J.-D. F., Sandlin, G. D., and Van Hoosier, M. E., 1978, *Astrophys. J.*, **226**, 687.
Kingston, A. E., Doyle, J. G., Dufton, P. L., and Gurman, J. B., 1982, *Solar Phys.*, **81**, 47.
Kneer, F. and Mattig, W., 1978, *Astron. Astrophys.*, **65**, 17.
Kneer, F., Scharmer, G., Mattig, W., Wyller, A., Artzner, G., Lemaire, P., and Vial, J. C., 1981, *Solar Phys.*, **69**, 289.
Krüger, A., Fürstenberg, F., Hildebrandt, J., and Staude, J., 1983, HHI-STP Report No. 14, Zentralinstitut für solar-terrestrische Physik Berlin (in press).
Kundu, M. R., Schmahl, E. J., and Gerassimenko, M., 1980, *Astron. Astrophys.*, **82**, 265.
Lang, K. R., and Willson, R. F., 1982, *Astrophys. J.*, **255**, L 111.
Lang, K. R., Willson, R. F., and Gaizauskas, V., 1983, ibid., (in press).
Lantos, P., 1968, *Ann. Astrophys.*, **31**, 105.
Levine, R. H., and Withbroe, G. L., 1977, *Solar Phys.*, **51**, 83.
Lites, B. W., and Skumanich, A., 1982, *Astrophys. J. Suppl.*, **49**, 293.
Livshits, M. A., Obridko, V. N., and Pikelner, S. B., 1966, *Astron. Zh.*, **43**, 1135.
Maltby, P., 1975, *Solar Phys.*, **43**, 91.
Maltby, P., 1977, *Solar Phys.*, **55**, 335.

Nicolas, K. R., Bartoe, J.-D. F., Brueckner, G. E., and Van Hoosier, M. E., 1979, *Astrophys. J.*, **233**, 741.
Nicolas, K. R., Kjeldseth-Moe, O., Bartoe, J.-D. F., and Brueckner, G. E., 1982, *Solar Phys.*, **81**, 253.
Obridko, V. N., 1979, *Astron. Zh.*, **56**, 67.
Pallavicini, R., Vaiana, G. S., Tofani, G., and Felli, M., 1979, *Astrophys. J.*, **229**, 375.
Pallavicini, R., Sakurai, T., and Vaiana, G. S., 1981, *Astron. Astrophys.*, **98**, 316.
Parkinson, J. H., 1973, *Solar Phys.*, **28**, 487.
Pye, J. P., Evans, K. D., Hutcheon, R. J., Gerassimenko, M., Davis, J. M., Krieger, A. S., and Vesecky, J. F., 1978, *Astron. Astrophys.*, **65**, 123.
Rosner, R., Tucker, W. H., and Vaiana, G. S., 1978, *Astrophys. J.*, **220**, 643.
Schmahl, E. J., Kundu, M. R., Strong, K. T., Bentley, R. D., Smith Jr., J. B., and Krall, K. R., 1982, *Solar Phys.* **80**, 233.
Seehafer, N., 1982, *Solar Phys.*, **81**, 69.
Seehafer, N., and Staude, J., 1979, *Astron. Nachr.*, **300**, 151.
Seehafer, N., and Staude, J., 1980, *Solar Phys.*, **67**, 121.
Staude, J., 1976, *Bull. Astron. Inst. Czechosl.*, **27**, 365.
— 1978, *ibid.*, **29**, 71.
— 1980, *Physica Solariterr.*, **14**, 58.
— 1981, *Astron. Astrophys.*, **100**, 284.
— 1983, HHI-STP Report No. 14, Zentralinstitut für solar-terrestrische Physik Berlin (in press).
Stellmacher, G., and Wiehr, E., 1975, *Astron. Astrophys.*, **45**, 69.
Sylwester, J., Schrijver, J., and Mewe, R., 1980, *Solar Phys.*, **67**, 285.
Teplitskaya, R. B., Grigoryeva, S. A., and Skochilov, V. G., 1977, *Issl. po geomagn., aeronomii i fizike Solntsa* **42**, 48.
Teplitskaya, R. B., Grigoryeva (Efendieva), S. A., and Skochilov, V. G., 1978, *Solar Phys.*, **56**, 293.
Urpo, S., Hildebrandt, J., Pflug, K., Staude, J. Fürstenberg, F., and Krüger, A., 1983, *Physica solariterr.* (in press).
Vesecky, J. F., Antiochos, S. K., and Underwood, J. H., 1979, *Astrophys. J.*, **233**, 987.
Withbroe, G. L., 1978, *Astrophys. J.*, **225**, 641.
Yun, H. S., Beebe, H. A., and Baggett, W. E., 1981, in: L. E. Cram and J. H. Thomas (eds.), *The Physics of Sunspots*, p. 142.
Zlotnik, E. Y., 1968, *Astron. Zh.*, **45**, 310, 585.
Žugžda, J. D., Locans, V., and Staude, J., 1983, *Solar Phys.*, **82**, 369.